Experimental investigation photoproduction processes on pion (H1, DESY).

More precise –

Exclusive rho meson photoproduction with a leading meutron at HERA.

On behalf of H1 Collaboration
Vazdik I.A.

DESY 15-123
August 2015

ISSN 0418-9833

Exclusive ρ^0 Meson Photoproduction with a Leading Neutron at HERA

H1 Collaboration

Abstract

A first measurement is presented of exclusive photoproduction of ρ^0 mesons associated with leading neutrons at HERA. The data were taken with the H1 detector in the years 2006 and 2007 at a centre-of-mass energy of $\sqrt{s} = 319$ GeV and correspond to an integrated luminosity of 1.16 pb^{-1}. The ρ^0 mesons with transverse momenta $p_T < 1$ GeV are reconstructed from their decays to charged pions, while leading neutrons carrying a large fraction of the incoming proton momentum, $x_L > 0.35$, are detected in the Forward Neutron Calorimeter. The phase space of the measurement is defined by the photon virtuality $Q^2 < 2$ GeV^2, the total energy of the photon-proton system $20 < W_{\gamma p} < 100$ GeV and the polar angle of the leading neutron $\theta_n < 0.75$ mrad. The cross section of the reaction $\gamma p \to \rho^0 n \pi^+$ is measured as a function of several variables. The data are interpreted in terms of a double peripheral process, involving pion exchange at the proton vertex followed by elastic photoproduction of a ρ^0 meson on the virtual pion. In the framework of one pion exchange dominance the elastic cross section of photon pion scattering, $\sigma^{el}(\gamma\pi^+ \to \rho^0\pi^+)$, is extracted. The value of this cross section indicates significant absorptive corrections for the exclusive reaction $\gamma p \to \rho^0 n \pi^+$.

Submitted to *Eur. Phys. J. C*

Eur. Phys. J. C (2016) 76:12
DOI 10.1140/epjc/s10052-015-3864-7

THE EUROPEAN PHYSICAL JOURNAL C

Regular Article - Experimental Physics

Exclusive ρ^0 meson photoproduction with a leading neutron at HERA

H1 Collaboration

V. Andreev[44], A. Baghdasaryan[33], K. Begzsuren[30], A. Belousov[24], A. Bolz[42], V. Boudry[24], G. Brandt[44], V. Brisson[23], D. Britzger[10], A. Buniatyan[2], A. Bylinkin[20,41], L. Bystritskaya[20], A. J. Campbell[10], K. B. Cantun Avila[19], K. Cerny[27], V. Chekelian[22], J. G. Contreras[19], J. Cvach[26], J. B. Dainton[16], K. Daum[32,37], C. Diaconu[18], M. Dobre[1], V. Dodonov[10], G. Eckerlin[10], S. Egli[31], E. Elsen[10], L. Favart[2], A. Fedotov[20], J. Feltesse[9], J. Ferencei[14], M. Fleischer[10], A. Fomenko[21], E. Gabathuler[16], J. Gayler[10], S. Ghazaryan[10], L. Goerlich[6], N. Gogitidze[21], M. Gouzevitch[38], C. Grab[25], A. Grebenyuk[5], T. Greenshaw[16], G. Grindhammer[22], D. Haidt[10], R. C. W. Henderson[15], J. Hladký[26], D. Hoffmann[18], R. Horisberger[31], T. Hreus[3], F. Huber[12], M. Jacquet[23], X. Janssen[3], H. Jung[5,10], M. Kapichine[8], C. Kiesling[22], M. Klein[16], C. Kleinwort[10], R. Kogler[11], P. Kostka[16], J. Kretzschmar[16], K. Krüger[10], M. P. J. Landon[17], W. Lange[34], P. Laycock[16], A. Lebedev[21], S. Levonian[10], K. Lipka[10], B. List[11], J. List[10], B. Lobodzinski[22], E. Malinovski[21], H-U. Martyn[1], S. J. Maxfield[16], A. Mehta[16], A. B. Meyer[10], H. Meyer[32], J. Meyer[10], S. Mikocki[6], A. Morozov[8], K. Müller[36], Th. Naumann[34], P. R. Newman[2], C. Niebuhr[10], G. Nowak[6], J. E. Olsson[10], D. Ozerov[10], C. Pascaud[23], G. D. Patel[16], E. Perez[39], A. Petrukhin[38], I. Picuric[25], H. Pirumov[18], D. Pitzl[10], R. Plačakytė[10], B. Pokorny[27], R. Polifka[27,42], B. Povh[13], V. Radescu[12], N. Raicevic[25], T. Ravdandorj[30], P. Reimer[26], E. Rizvi[17], P. Robmann[36], R. Roosen[3], A. Rostovtsev[15], M. Rotaru[1], S. Rusakov[21,*], D. Šálek[27], D. P. C. Sankey[4], M. Sauter[12], E. Sauvan[18,43], S. Schmitt[10,a], L. Schoeffel[9], A. Schöning[12], F. Sefkow[10], S. Shushkevich[10], Y. Soloviev[10,21], P. Sopicki[6], D. South[10], V. Spaskov[8], A. Specka[24], M. Steder[10], B. Stella[28], U. Straumann[36], T. Sykora[3,27], P. D. Thompson[2], D. Traynor[17], P. Truöl[36], I. Tsakov[29], B. Tseepeldorj[30,40], J. Turnau[6], A. Valkárová[27], C. Vallée[18], P. Van Mechelen[3], Y. Vazdik[21], D. Wegener[7], E. Wünsch[10], J. Žáček[27], Z. Zhang[23], R. Žlebčík[27], H. Zohrabyan[53], F. Zomer[23]

[1] Physikalisches Institut der RWTH, Aachen, Germany
[2] School of Physics and Astronomy, University of Birmingham, Birmingham, UK[b]
[3] Inter-University Institute for High Energies ULB-VUB, Brussels and Universiteit Antwerpen, Antwerp, Belgium[c]
[4] Horia Hulubei National Institute for R&D in Physics and Nuclear Engineering (HH-NIPNE/IFIN-HH), Bucharest, Romania[b]
[5] STFC, Rutherford Appleton Laboratory, Didcot, Oxfordshire, UK[b]
[6] Institute of Nuclear Physics, Polish Academy of Sciences, 31-342 Kraków, Poland[e]
[7] Institut für Physik, TU Dortmund, Dortmund, Germany[f]
[8] Joint Institute for Nuclear Research, Dubna, Russia
[9] Irfu/SPP, CE Saclay, Gif-sur-Yvette Cedex, France
[10] DESY, Hamburg, Germany
[11] Institut für Experimentalphysik, Universität Hamburg, Hamburg, Germany[f]
[12] Physikalisches Institut, Universität Heidelberg, Heidelberg, Germany[f]
[13] Max-Planck-Institut für Kernphysik, Heidelberg, Germany
[14] Institute of Experimental Physics, Slovak Academy of Sciences, Košice, Slovak Republic[g]
[15] Department of Physics, University of Lancaster, Lancaster, UK[b]
[16] Department of Physics, University of Liverpool, Liverpool, UK[b]
[17] School of Physics and Astronomy, Queen Mary, University of London, London, UK[b]
[18] Aix Marseille Université, CNRS/IN2P3, CPPM UMR 7346, 13288 Marseille, France
[19] Departamento de Física Aplicada, CINVESTAV, Mérida, Yucatán, Mexico[i]
[20] Institute for Theoretical and Experimental Physics, Moscow, Russia[j]
[21] Lebedev Physical Institute, Moscow, Russia
[22] Max-Planck-Institut für Physik, Munich, Germany
[23] LAL, Université Paris-Sud, CNRS/IN2P3, Orsay, France
[24] LLR, Ecole Polytechnique, CNRS/IN2P3, Palaiseau, France
[25] Faculty of Science, University of Montenegro, Podgorica, Montenegro[b]
[26] Institute of Physics, Academy of Sciences of the Czech Republic, Prague, Czech Republic[k]
[27] Faculty of Mathematics and Physics, Charles University, Prague, Czech Republic[k]
[28] Dipartimento di Fisica, Università di Roma Tre and INFN Roma 3, Rome, Italy
[29] Institute for Nuclear Research and Nuclear Energy, Sofia, Bulgaria

HERA: The World's Only ep Collider

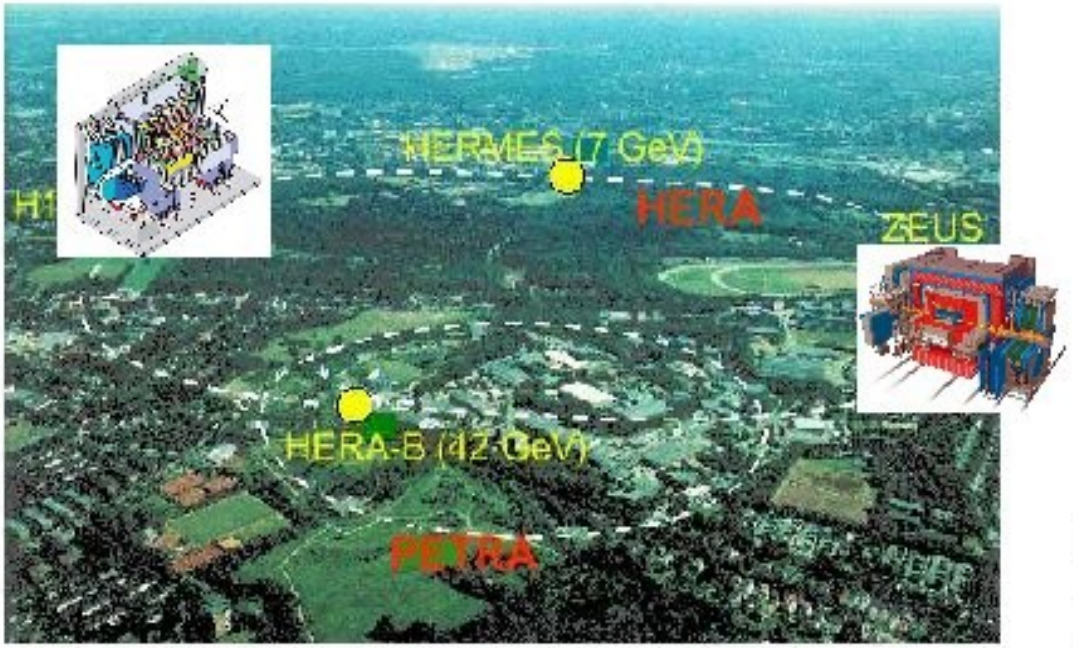

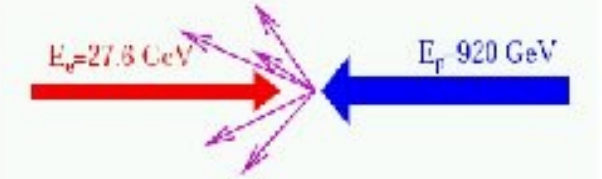

- 1998 E_p upgrade: 820 $\Rightarrow$ 920 GeV
  ($\sqrt{s}$: 301 $\Rightarrow$ 319 GeV)
- 2001 HERA-2 upgrade: $\mathcal{L} \times 3$, Polarised e^-/e^+
  ($\langle P \rangle = 40\%$)

HERA-1 (1993-2000) $\simeq 120\ \mathrm{pb}^{-1}$

HERA-2 (2003-2007) $\simeq 380\ \mathrm{pb}^{-1}$

Final Data samples
H1+ZEUS: $2 \times 0.5\ \mathrm{fb}^{-1}$

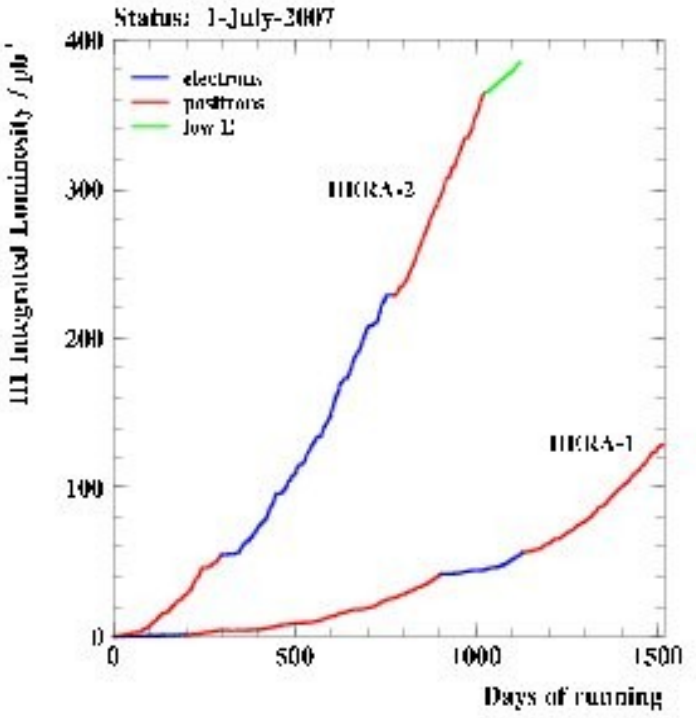

History -

G.F. Chew and F.E.Low Phys.Rev. 113,1640, 1959
C.Goebel Phys.Rev.Lett vol 1 p337 1958

Mainly reaction – pi +N --> pi + pi + N

Example - JETF v45, p913, 1963
Cross-section pi+ pi- --> pi+ pi- = 34 +- 9 mb
(energy in cms = 4-7 Mpi)

FIAN – 1988, v 186 p 106
Gamma + p --> gamma' + pi+ neutron
Cross-section gamma-pi+ = (5.4+-1.) 10**(-32) cm**2/st
Egm=650 mev, s1=6.5mpi
alfa(pi+) = -beta(pi+) = (20 =-12) 10**(-43) cm**3

UCRL-8427

UNSTABLE PARTICLES AS TARGETS IN SCATTERING EXPERIMENTS

G. F. Chew

Radiation Laboratory
University of California
Berkeley, California

and

F. E. Low

Radiation Laboratory, University of California
Berkeley, California
and
Department of Physics and Laboratory for Nuclear Science
Massachusetts Institute of Technology
Cambridge, Massachusetts

August 21, 1959

ABSTRACT

A general method is suggested for analyzing the scattering of particle A by particle B, leading to three or more final particles, in order to obtain the cross section for the interaction of A with a particle which is virtually contained in B. Binding complications are absent if a plausible assumption about the location and residues of poles in the S-matrix is accepted. The method is useful for unstable particles from which free targets cannot be made; the special examples of pion and neutron targets are discussed in detail.

mation (Tamm-Dancoff), one finds that the P-wave amplitudes are predicted to be negative, and the positive D-wave amplitude is very small up to at least a Bev.[7]

(b') The large value of the meson production cross section near threshold in the $I=\frac{1}{2}$ state,[6] but not in the $I=\frac{3}{2}$ state. In the latter case the observed production cross section is roughly in agreement with static model calculations, but these are a factor of about 5 too small in the $I=\frac{1}{2}$ state.[7]

(c) The maximum of the total cross section in the $I=\frac{3}{2}$ state at ~0.9 Bev (the "second maximum".[5] It was suggested that this reflected a resonance in the π-π scattering,[6] but it was subsequently pointed out that the spread of momentum of the self-field pions would make the resulting maximum in the π-N cross section very broad.[8] Further, there is no evidence that the final pair of pions tend to have the presumed resonant relative energy. But at this energy the final state resonant π-N interaction is probably important, as well as perhaps "multiple scattering" in the self field, so that the situation is too involved to allow ruling out of this mechanism. For instance, if the π-N resonant final state is indeed important, this may tend to select the momentum of the virtual pion, so that the effective momentum spread is really less.

(d) The large size of the high-energy total cross section, and the consequent backward peaking of the nucleon's angular distribution, in both elastic and inelastic events of low multiplicity.[5] This clearly indicates that the incident π interacts with the virtual pion cloud of the nucleon, rather than with a core.

A way of getting a quantitative estimate of the π-π interaction strength is by isolating the contribution of the one-pion exchange diagram (Fig. 1) from all others. One can attempt to do this by using the fact that this matrix element becomes infinite when the exchanged pion is real, i.e., for a momentum transfer Δ to the nucleon of about μ. One cannot of course reach this physically, but one can try to extrapolate the cross section as a function of Δ^2 to $\Delta^2=-\mu^2$. This is just the principle of the threshold theorem, used for instance in the determination of the π-N coupling constant from π-N scattering. Chew[9] has recently suggested the application of the extrapolation procedure to a determination of the π-N coupling constant from N-N scattering. The present case is similar, but in order to deduce the dependence of the matrix element on momentum transfer, one must extract from the cross

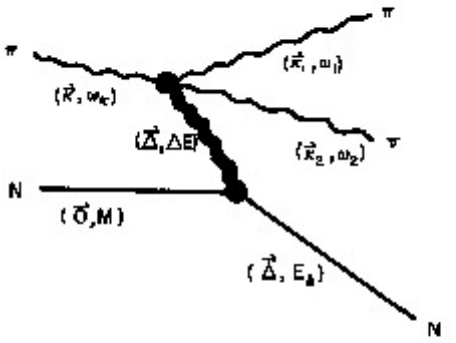

FIG. 1. Feynman diagram of the pole-containing matrix element. Beneath each line is written its momentum and energy.

section the phase space of the three-body final state.[10]

It is convenient to work in the laboratory system. We have, for the differential cross section for single pion production,

$$d\sigma=(2\pi)^4 |\mathfrak{M}|^2 d^3k_1 d^3k_2 \delta(\omega_k+\omega_p+E_\Delta-W), \quad (1)$$

where $W=\omega_k+M$ the total energy, and we have put the velocity of the incident pion equal to unity. The pole obviously occurs at $T_\Delta=-\mu^2/2M$ where $T_\Delta=E_\Delta-M$, the kinetic energy of the final nucleon. It is convenient to describe the final state by the relative momentum of the final mesons (in their center of mass) $\vec{\xi}$ and the total momentum of the mesons $\vec{P}$ or, equivalently, the momentum $\vec{\Delta}$ of the nucleon. The pertinent Jacobian is

$$d^3k_1 d^3k_2 = d^3\xi d^3P \frac{1}{\omega_\xi \Omega_\xi}\left[\xi_\xi^2 - \frac{(\vec{\xi}\cdot\vec{P})^2}{4\omega_\xi^2}\right],$$

where

$$\omega_\xi^2=\xi^2-\mu^2, \Omega_\xi^2=\omega_\xi^2+P^2/4. \quad (2)$$

Integrating over the direction of $\vec{\xi}$ (the length is fixed by energy conservation), we find that Eq. (1) becomes

$$d\sigma=8\pi^5 |\mathfrak{M}|^2 \omega_\xi |(W-E_\Delta)^2-v_\xi^2 P^2/3| d^3\Delta, \quad (3)$$

where

$$v_\xi=\frac{1}{\omega_\xi}=\left(\frac{\vec{k}\cdot\vec{\Delta}-WT_\Delta-\frac{1}{2}\mu^2}{\vec{k}\cdot\vec{\Delta}-WT_\Delta+\frac{1}{2}\mu^2}\right)^{1/2}. \quad (4)$$

The $|\ |^2$ on $|\mathfrak{M}|^2$ indicate an average. Finally,

Proposal for a Forward Neutron Calorimeter for the H1 Experiment at DESY

H1-Collaboration *
M. Beck, W. Brückner, Th. Haller, D.M. Jansen, F. Metlica,
T. Nunnemann, B. Povh, R. Todenhagen
Max-Planck Institut für Kernphysik, Postfach 103980,
69029 Heidelberg, Germany
(August 7, 1995)

Abstract

At HERA, the reaction $ep \to e'nX$ can be studied. In a properly chosen kinematic domain, it is expected that this reaction will be dominated by deep inelastic scattering (DIS) on a pion coupled to the ground state or excited states of the proton. A forward neutron calorimeter in conjunction with the H1 experiment at HERA, can be used to study these interactions and to measure the pion structure function. In addition, the fraction of large rapidity-gap events ascribed to pion exchange can be measured. A proposal for installation of a forward neutron calorimeter for the H1 Experiment at DESY is described in this paper.

Introduction

We propose to add a new forward neutron calorimeter to the H1 experiment at DESY. The purpose of the new neutron calorimeter is to measure the energy and angle of produced neutrons with high precision. The calorimeter will be situated 107 m from the interaction point at zero degrees with respect to the incident proton direction. Measurement of the forward neutron angle and energy, along with the determination of the scattered electron and the hadronic jets, will to a large extent specify the kinematics of the reaction $ep \to e'nX$. This paper describes the physics motivation and design specifications for the neutron calorimeter.

Physics Motivation

Many theoretical papers have discussed the possibility of measuring the pion structure function at HERA [1–5]. The pion cloud around the nucleon can contribute to the deep

*Subject to approval by the collaboration board on September 6, 1995

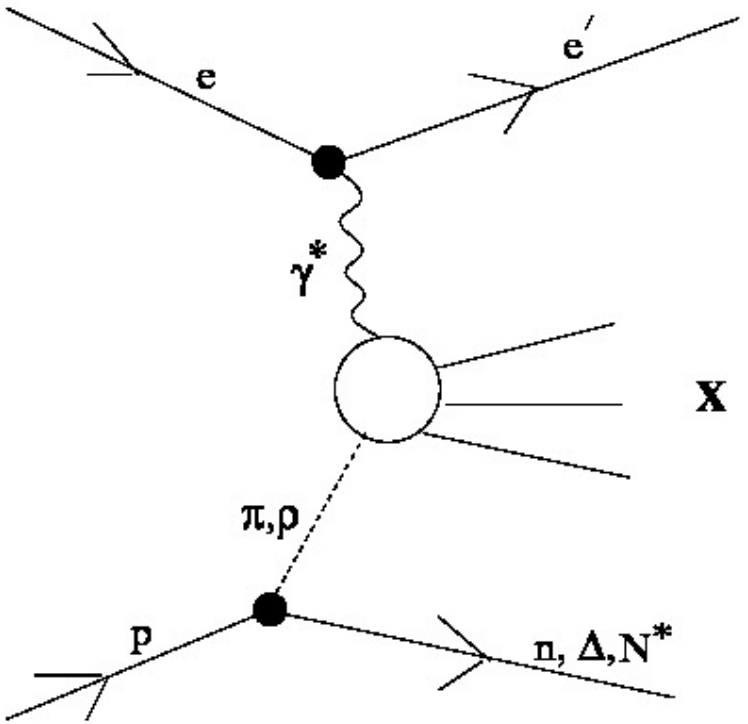

FIG. 1. The pion exchange contribution to deep inelastic scattering.

The H1 detector at the e-p storage ring HERA

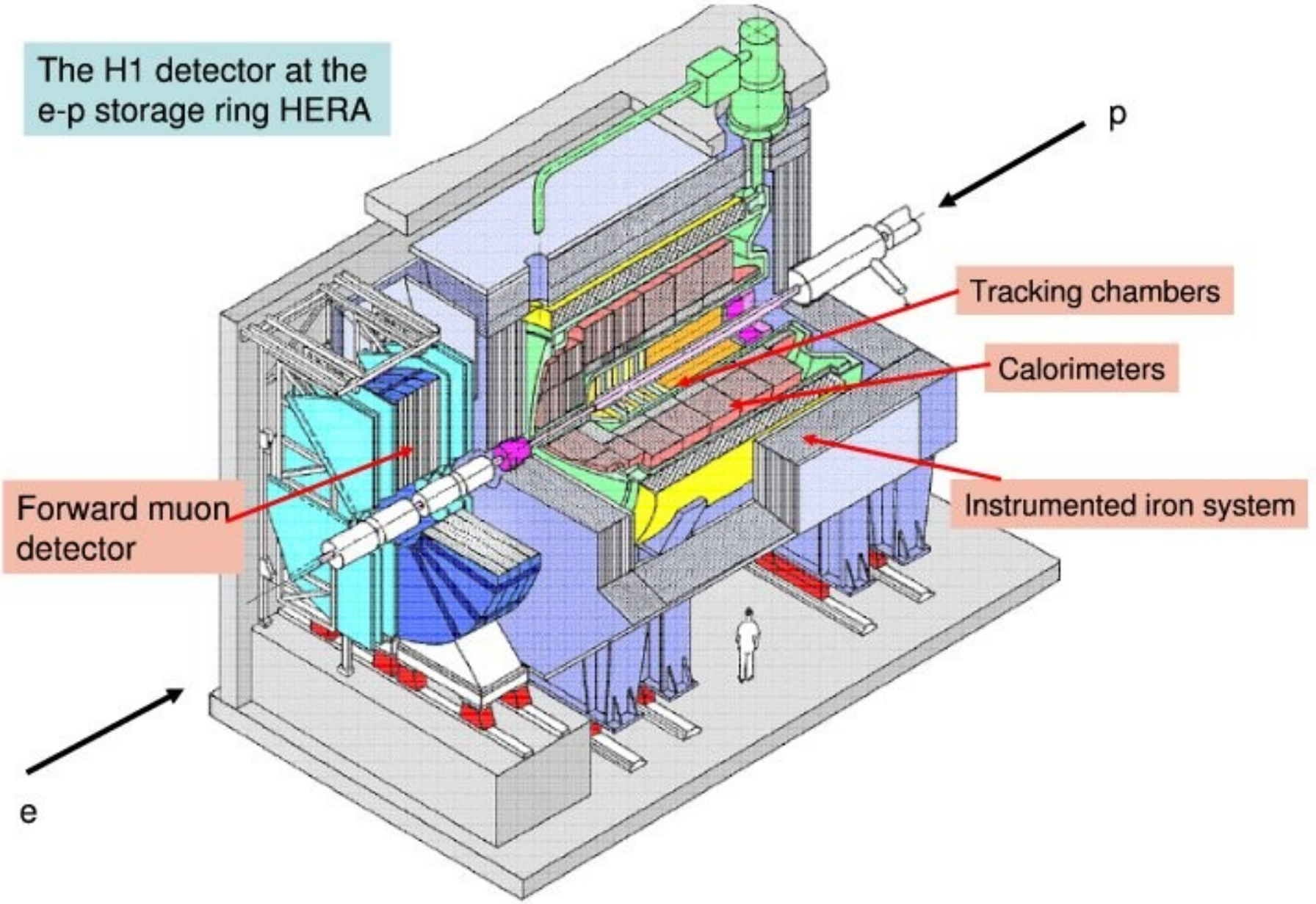

3

Side view

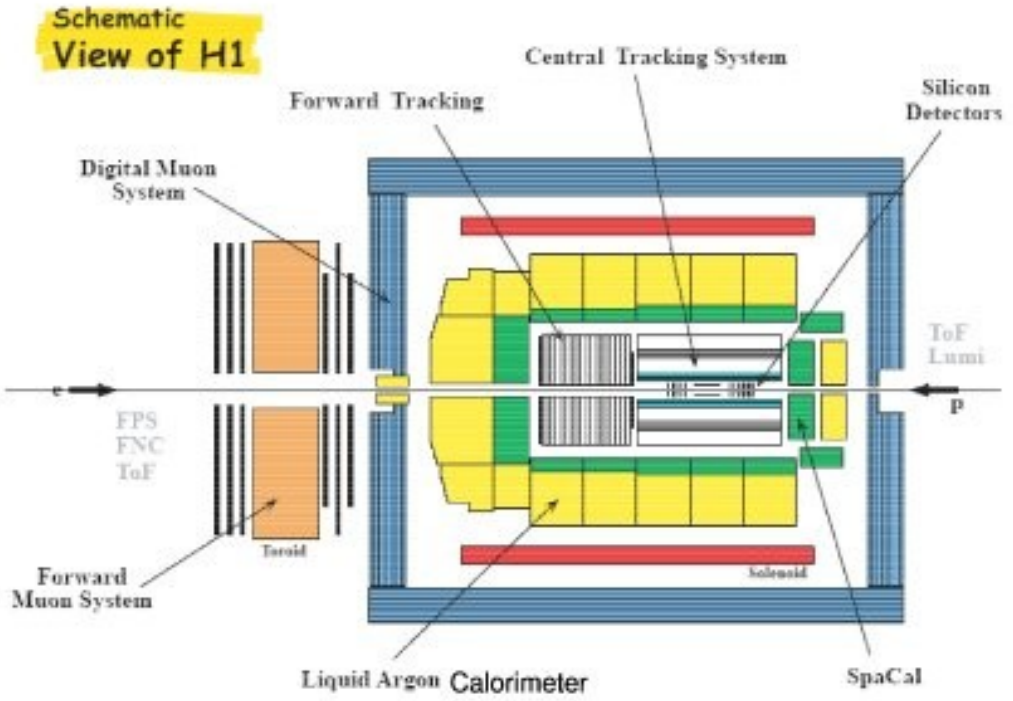
Schematic
View of H1
Central Tracking System
Forward Tracking
Silicon
Detectors
Digital Muon
System
ToF
Lumi
e
p
FPS
FNC
ToF
Toroid
Solenoid
Forward
Muon System
Liquid Argon Calorimeter
SpaCal

Introduction

- First observation of exclusive photoproduction on (virtual) pion
  - Unique for HERA (before that γ, π beams did exist, but no target)
  - Extends further (very powerful) VM field at HERA

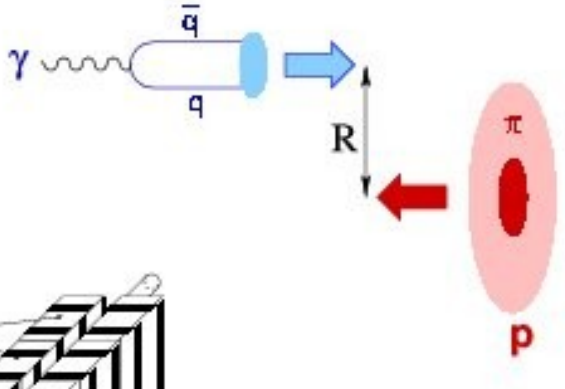

- Key observables:
  - $x_L = E_n/E_p$ (or $x_\pi = 1 - x_L$) distribution: $\sim f_{\pi/p}(x_L)$
  - W dependence: $\sim W^\delta$ – nature of exchange object(s)
  - t-slope of ρ^0 ($b \propto R^2$ in geometric picture)

- Main experimental difficulty:
  - Trigger (tagged γp – too large W to observe VM;
    untagged γp – too high rates/prescales)
  - Limited acceptance for forward π and N ($\eta_{\rm lab} \geq 6$)

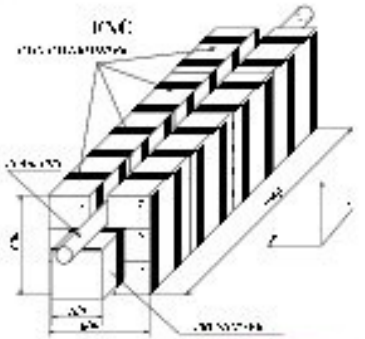

- Advantages of H1@HERA2
  - Improved FNC (distinguish and measure n and γ/π^0)
  - Powerful fast track trigger
    (allows untagged soft γp to be collected)

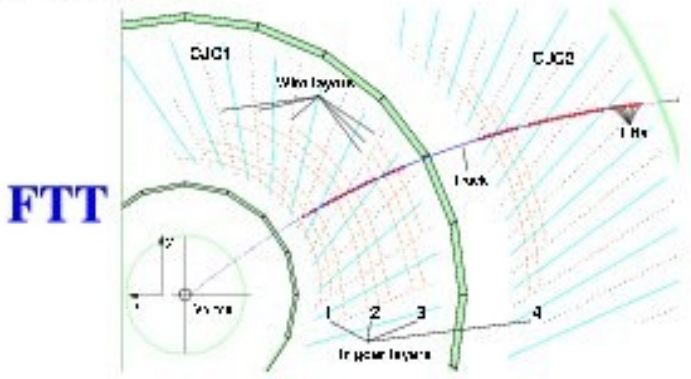

Reaction of interest and the analysis phase space

$$\gamma^* + p \rightarrow \rho^0 \pi^+ n$$

$$\rho^0 \rightarrow \pi^+\pi^-$$

Photoproduction:	$Q^2 < 2$ GeV^2	($\langle Q^2 \rangle = 0.05$ GeV^2)
Low p_t:	$\lvert t \rvert < 1$ GeV^2	($\langle \lvert t \rvert \rangle = 0.20$ GeV^2)
Small mass:	$0.3 < m_{\pi\pi} < 1.5$ GeV	(m_{ρ^0})
$\pi^{\mid}, \pi$ in CT:	$20 < W_{\gamma p} < 100$ GeV	($\langle W_{\gamma p} \rangle = 48$ GeV)
Leading n:	$E_n > 120$ GeV;	$\theta_n < 0.75$ mrad

No hard scale present $\Rightarrow$ Regge framework is most appropriate

Contributing processes and their modelling

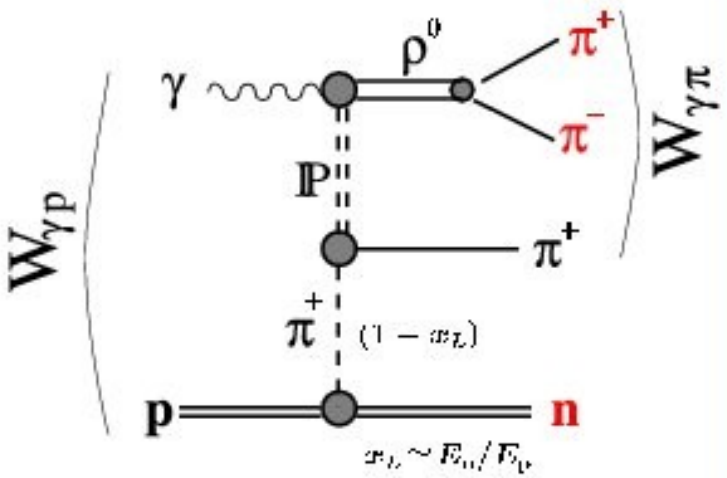

Pompyt × Pythia6

(π-flux) (elastic $\gamma\pi \to \rho^0\pi$)

Signal (DPP)

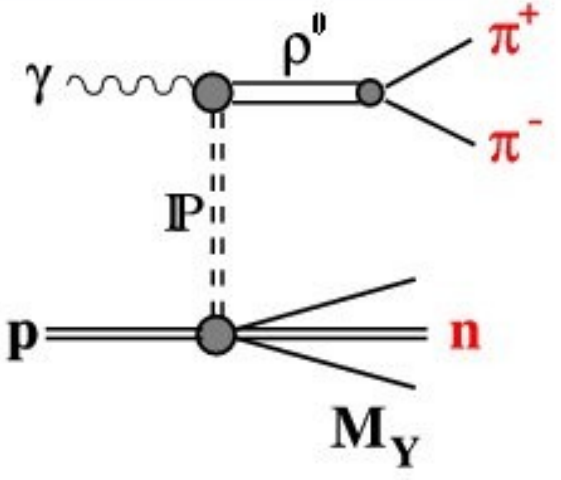

DiffVM

(elastic, p-diss, γ-diss, double diss)

Background

$W_{\gamma p} \simeq \sqrt{2(E-p_z)_p E_p}$

$W_{\gamma\pi} \simeq W_{\gamma p}\sqrt{1-x_L}$

- DPP expectations: $f_{\pi/p}(x_L,t) \to x_L$ shape, $p^2_{t,p}$ slope, $b - b_{eff}(M_{\pi N})$
- Diffractive bgr is well known (but has an irreducible part: $M_Y = N^* \to n\pi$)

Typical Event

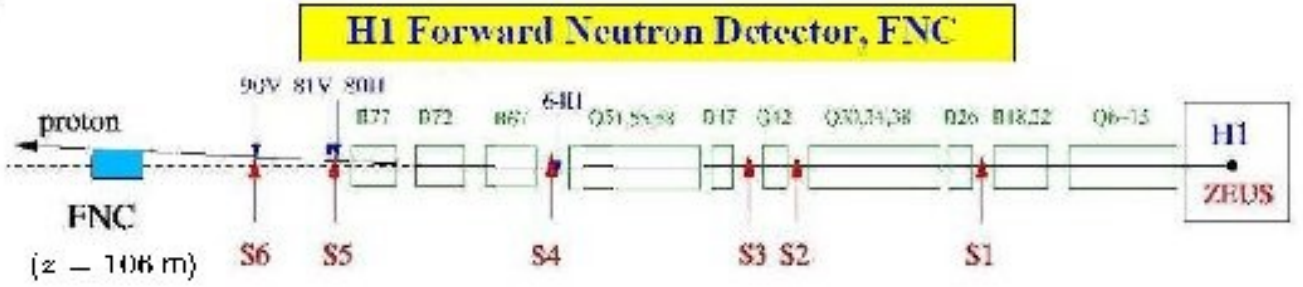

Key Experimental Ingredients

Improved H1 FNC (distinguish $\langle P \rangle = 98\%$) and measure n and γ/π^0)

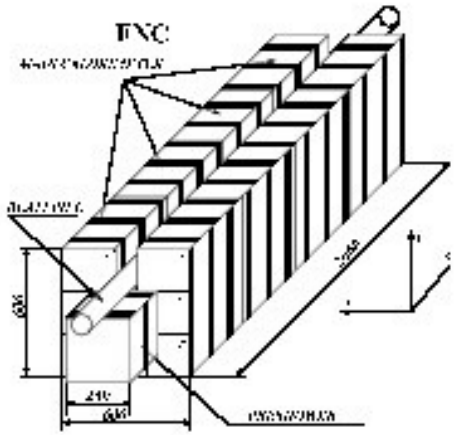

located at $z = 106$m from IP

$\langle A \rangle \simeq 30\%$ for $\theta < 0.8$ mrad

Preshower: $60X_0$, Main Calo: 8.9λ

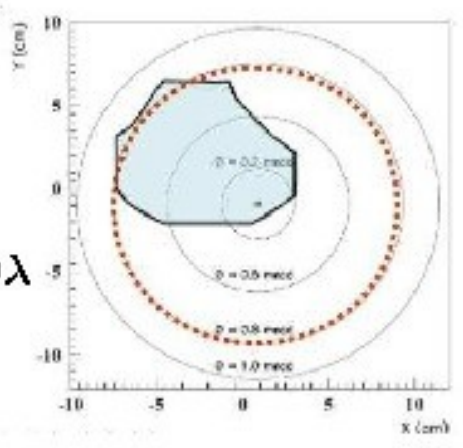

Powerful fast track trigger (allows untagged soft γp to be collected)

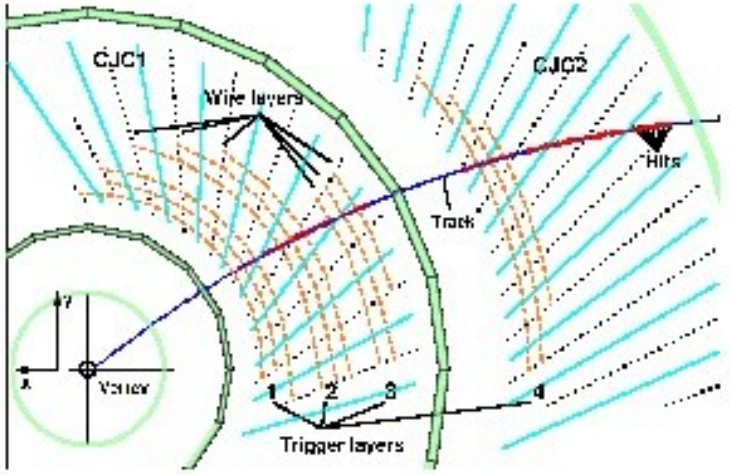

Analysis Summary

- **Data sample**
  - $2006-2007e^+$ runs. $\sqrt{s}=319$ GeV, $\mathcal{L}=1.16$ pb^{-1} $\sim$ 6600 events in final sample
  - Trigger: $\langle\epsilon_{L1}\rangle \simeq 0.8$, $\langle\epsilon_{L2}\rangle \simeq 1.0$
- **Tracking**
  - 2 tracks with $p_t^{tr}>0.2$ GeV, $20^o<\theta^{tr}<160^o$ fitted to event vertex $z_{vtx}|<30$ cm, net charge $=0$
  - Effective mass range: $0.6<M_{\pi\pi}<1.1$ GeV (analysis): $\Rightarrow \sigma(\rho^0)$ for $0.28<M_{\pi\pi}<1.5$ GeV
- **FNC**
  - High energy neutron, $E_n>120$ GeV, within good acceptance region: $\theta_n<0.75$ mrad
  - Background fraction determined from x_L shape: $F_{bg}=0.36\pm0.06$ (subtracted from the data)
- **Exclusivity**
  - Nothing above noise level in the detector except two tracks from ρ^0 decay and the leading neutron
- **Cross section measurement phase space and precision**
  - Photoproduction: $Q^2<2$ GeV^2, $20<W_{\gamma p}<100$ GeV
  - Leading neutron: $0.35<x_L<0.95$, $p_{t,n}<x_L\cdot 0.69$ GeV
  - ρ^0 meson: $0.28<M_{\pi\pi}<1.5$ GeV, $p_{t,\rho}<1$ GeV

$$\delta_{stat}=2.1\% \oplus \delta_{sys}=15.5\% \oplus \delta_{norm}=5.9\% \Rightarrow \delta_{tot}=16.6\%$$

ρ-meson shape

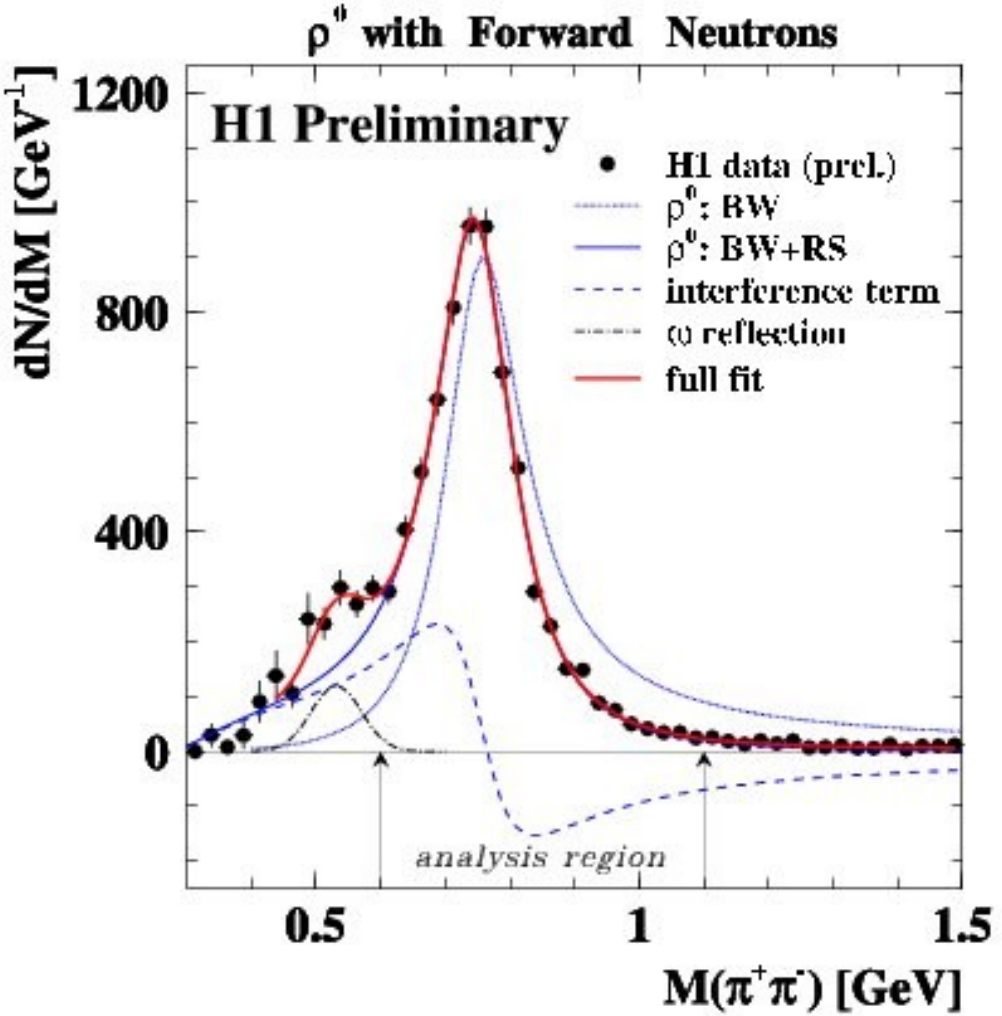

$$\frac{dN(M_{\pi\pi})}{dM_{\pi\pi}} \propto BW_\rho(M_{\pi\pi}) \left(\frac{M_\rho}{M_{\pi\pi}}\right)^{n_{RS}}$$

$$M = 764 \pm 3 \text{ MeV}$$

$$\Gamma = 154 \pm 5 \text{ MeV}$$

$$n_{RS} = 4.17 \pm 0.27$$

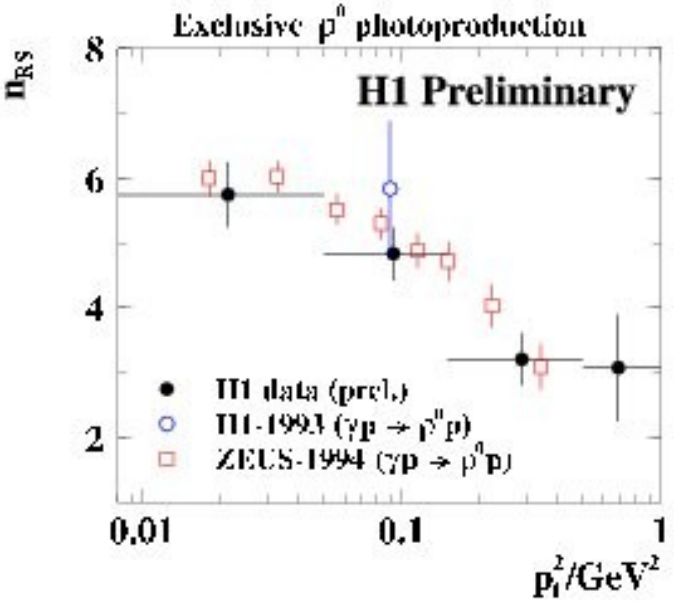

Analysis region: $0.6 < M_{\pi\ \pi} < 1.1$ GeV extrapolated using BW to the full range: $0.28 < M_{\rho^0} < 1.5$ GeV

Control Plots for basic kinematics

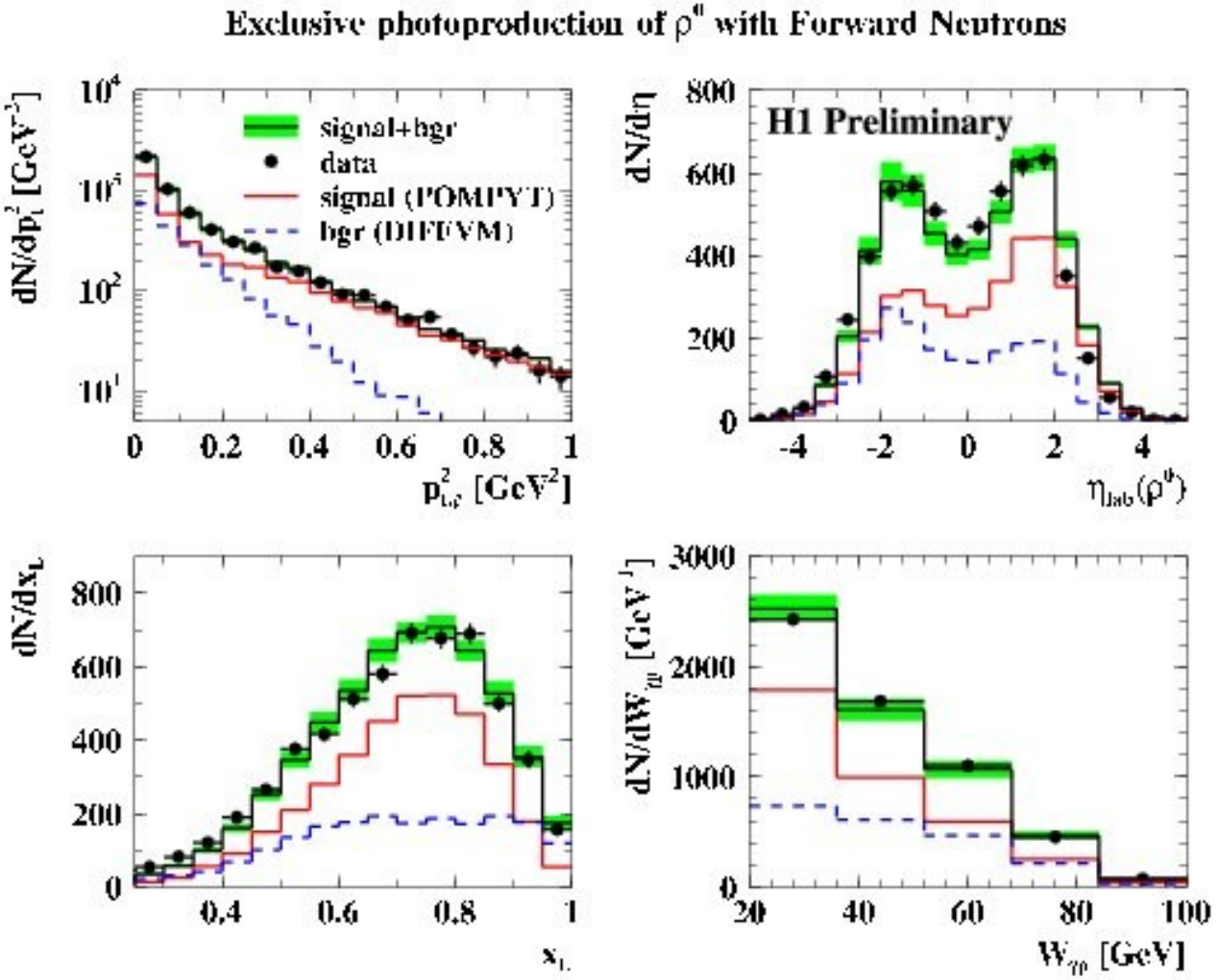

Data points are shown with stat. errors only; green band represents estimated bgr fraction uncertainty

OPE and pion fluxes

$$\frac{d^2\sigma_{\gamma p}(W^2,x_L,t)}{dx_L dt} = f_{\pi/p}(x_L,t)\sigma_{\gamma\pi}((1-x_L)W^2)$$

$$\frac{d\sigma_{\gamma p}}{dx_L} = \int_{t_0(x_L)}^{t_{min}(x_L)} f_{\pi/p}(x_L,t)dt \cdot \sigma_{\gamma\pi}(W_{\gamma\pi})$$

where $t = -\frac{p_{T,n}^2}{x_L} - \frac{(1-x_L)(m_n^2 - m_p^2 x_L)}{x_L}$

$$\sigma_{\gamma\pi}(W_{\gamma\pi}) = \frac{1}{\Gamma_\pi(x_L)}\frac{d\sigma_{\gamma p}}{dx_L} \quad \text{and} \quad \overline{\sigma_{\gamma\pi}}(\langle W_{\gamma\pi}\rangle) = \frac{\sigma_{\gamma p}}{\int \Gamma_\pi}$$

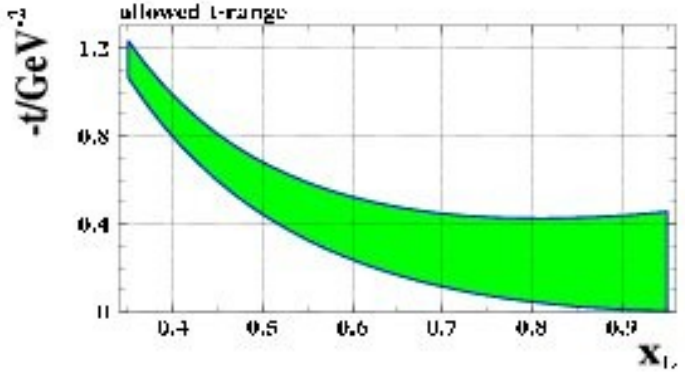

Problem: too many different fluxes on the market

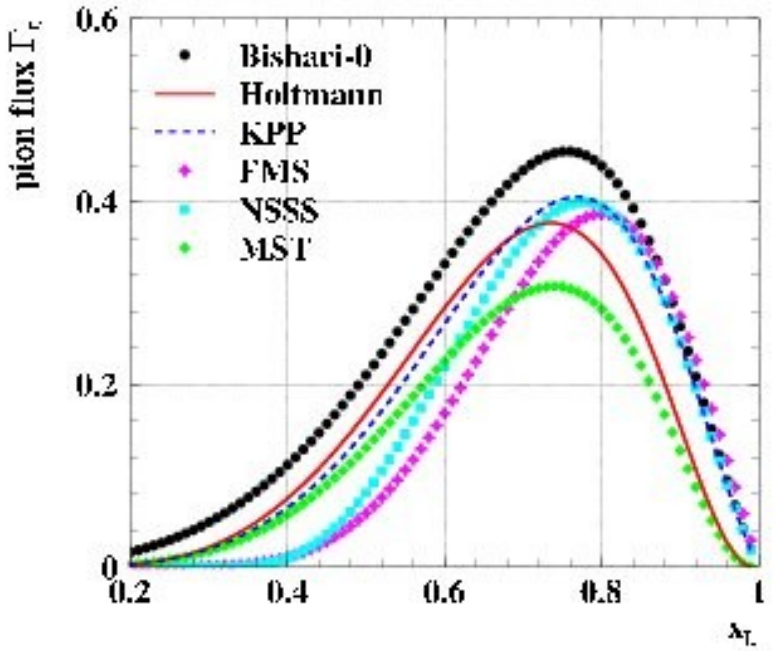

Typical examples:

$$f_{\pi^+/p}(x_L,t) = \frac{1}{2\pi}\frac{g_{p\pi n}^2}{4\pi}(1-x_L)\frac{-t}{(m_\pi^2 - t)^2}\exp[-R_{\pi n}^2\frac{m_n^2 - t}{1 - x_L}]$$ – H. Holtmann et al., *Nucl. Phys.* A596 (1996) 631.

$$f_{\pi^+/p}(x_L,t) = \frac{1}{2\pi}\frac{g_{p\pi n}^2}{4\pi}(1-x_L)^{1-2\alpha' t}\frac{-t}{(m_\pi^2 - t)^2}\exp[-R_\pi^2(m_\pi^2 - t)]$$ – B. Kopeliovich et al., *Z. Phys.* C73 (1996) 125.

Pion fluxes confronted with H1 data

Make restricted selection of π-fluxes on the basis of shape comparison only

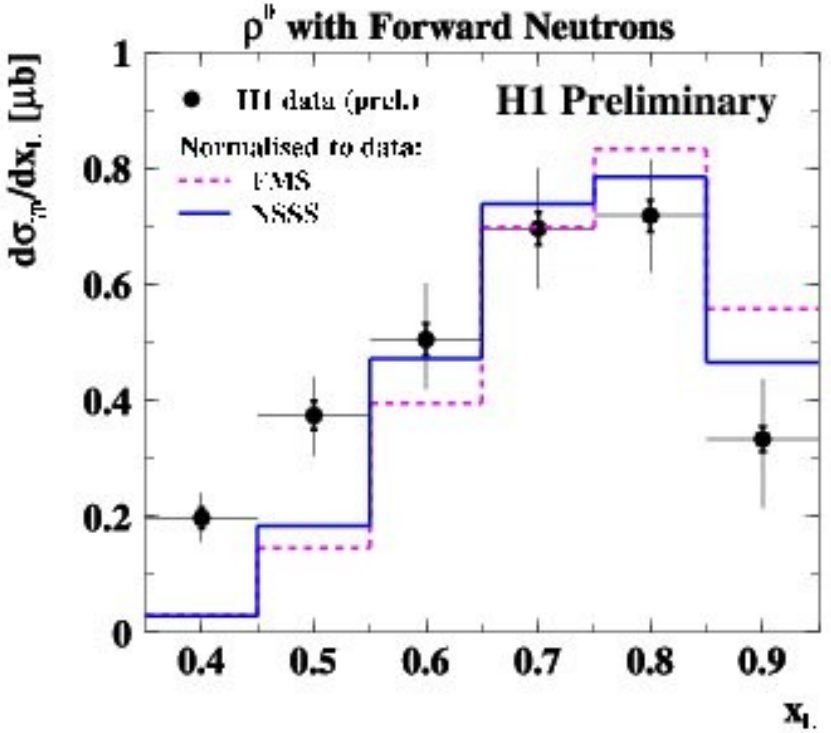

Example of fluxes excluded by the data
(too soft pions 'in the proton')

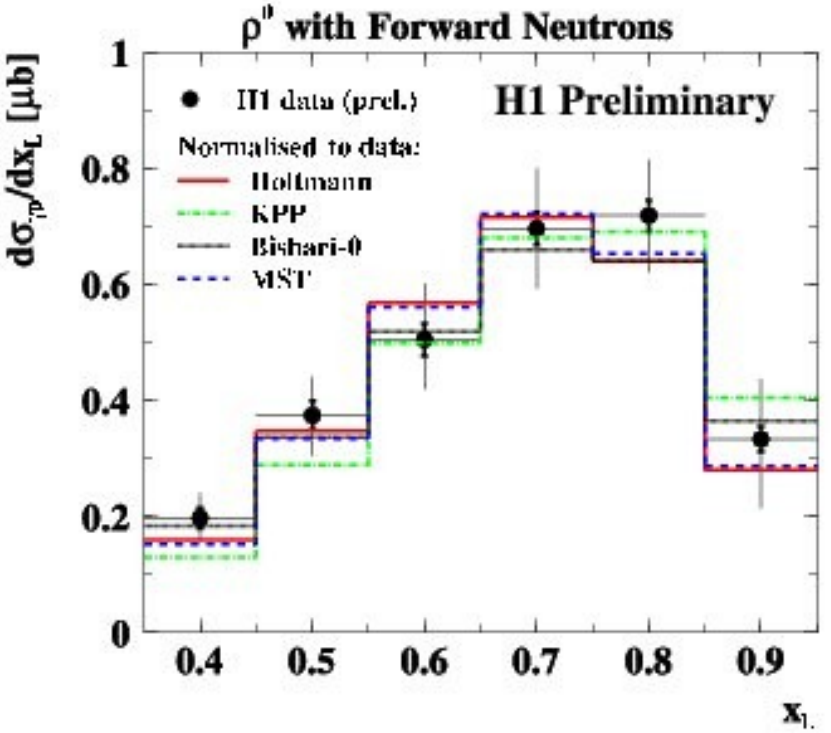

Fluxes compatible with H1 data

Total cross sections

$$\sigma_{\gamma p} = \frac{\sigma_{ep}}{\int f_{\gamma/e}(y,Q^2)\mathrm{d}y\mathrm{d}Q^2} = \frac{N_{\mathrm{data}} - N_{\mathrm{bgr}}}{\mathcal{L}(A\cdot\epsilon)\mathcal{F}}\cdot C_\rho$$

Where

- N_{bgr} – diffractive dissociation bgr from MC
- $\mathcal{L}$ – integrated luminosity
- $A\cdot\epsilon$ – correction for detector acceptance and efficiency
- $\mathcal{F}$ – photon flux integrated over kinematic domain $20 < W < 100$ GeV, $Q^2 < 2$ GeV^2
- C_ρ – numerical factor accounting for extrapolation to full ρ^0 mass range

For OPE dominated range, $0.35 < x_L < 0.95$, and $20 < W_{\gamma p} < 100$ GeV, $\theta_n < 0.75$ mrad

$$\sigma(\gamma p \to \rho^0 n(\pi^+)) = (280 \pm 6_{\mathrm{stat}} \pm 46_{\mathrm{sys}})\ \mathrm{nb}$$

$$\sigma_{\gamma\pi}(\langle W_{\gamma\pi}\rangle) = \frac{\sigma_{\gamma p}}{\int f_{\pi^+/p}(x_L,t)dx_L dt},$$

and for $\langle W_{\gamma\pi}\rangle = 22$ GeV

$$\sigma_{\mathrm{el}}(\gamma\pi^+ \to \rho^0\pi^+) = (2.03 \pm 0.34_{\mathrm{exp}} \pm 0.51_{\mathrm{model}})\ \mu\mathrm{b}$$

Taking interpolated value of $\sigma(\gamma p \to \rho^0 p) = 9.5 = 0.5\ \mu$b at corresponding energy, we obtain

$$r_{\mathrm{el}} = \sigma^{\mathrm{el}}_{\gamma\pi}/\sigma^{\mathrm{el}}_{\gamma p} = 0.21 \pm 0.06$$

(cf. r_{el} $\sigma^{\mathrm{tot}}_{\gamma\pi}/\sigma^{\mathrm{tot}}_{\gamma p}$ 0.32 ± 0.03 [ZEUS, 2002])

Total γp and $\gamma\pi$ cross sections

Inner error bars – statistical uncertainty
outer error bars – $\sqrt{\text{stat}^2 + \text{sys}^2}$

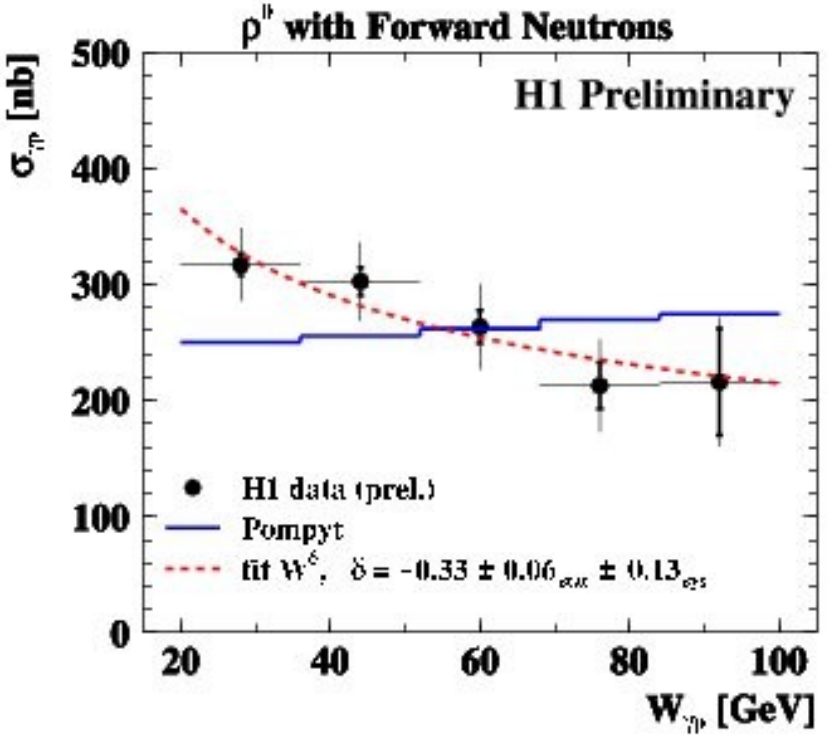

Regge motivated power low fit W^{δ} yields $\delta < 0$

Inner error bars – total experimental uncertainty
outer error bars – $\sqrt{\text{exp}^2 + \text{model}^2}$

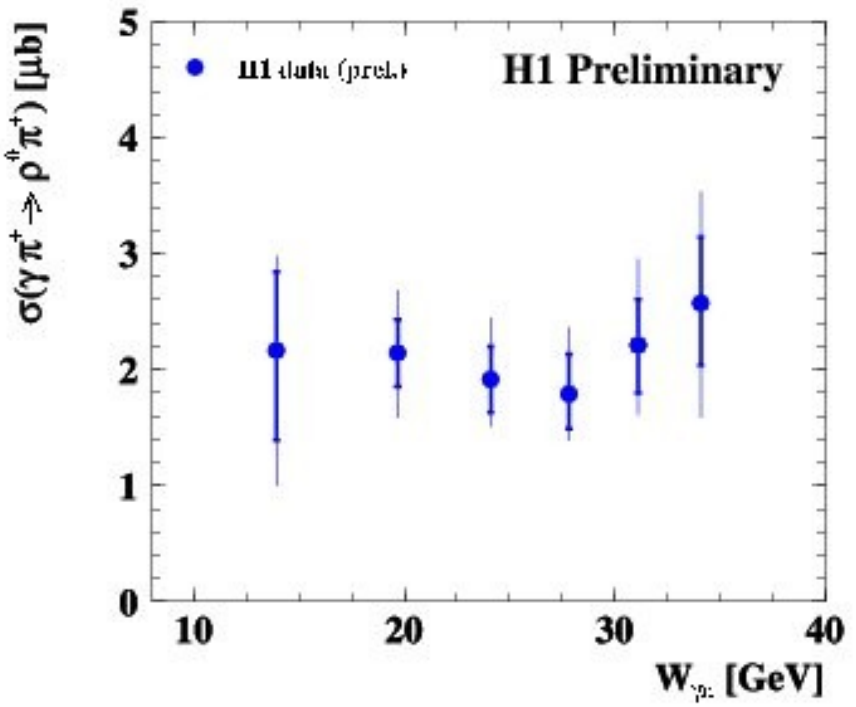

Holtmann flux is used for the central values.

Model uncertainty $\sim 25\%$

Differential cross sections in η

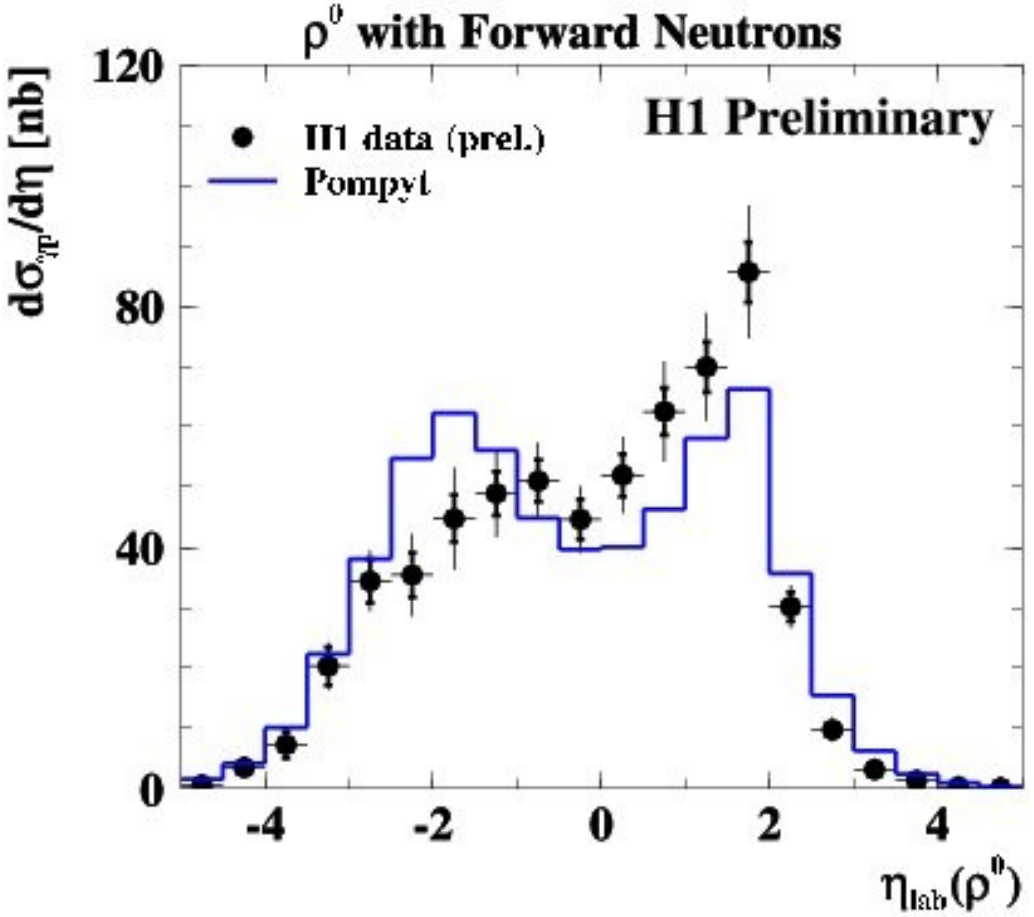

Different energy dependence in data and MC is also reflected in η shape

Differential cross section in p_t^2

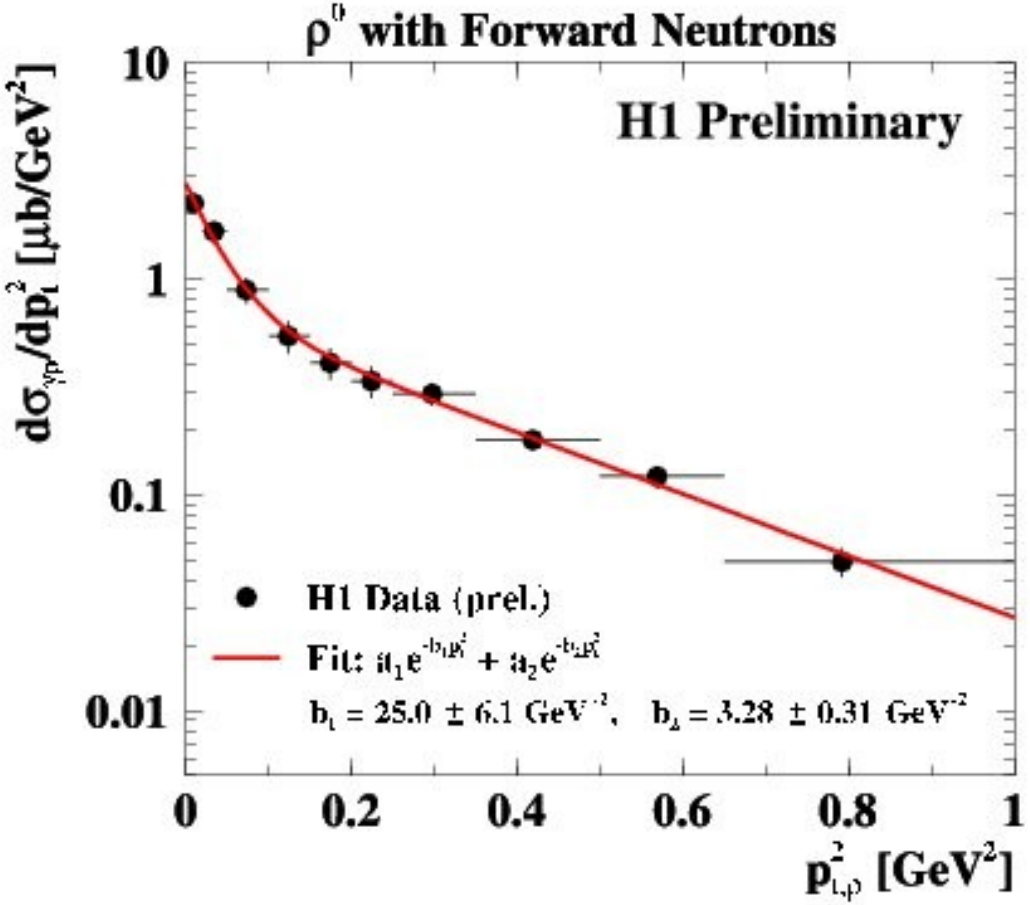

N.P.Zotov, V.A.Tsarev - 1978

Soviet Journal of Particles and Nuclei 9(3)266-290

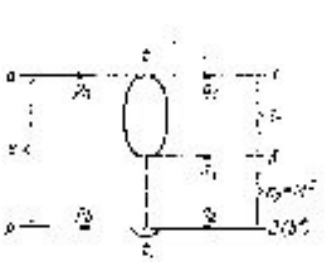

DPP $2 \to 3$

ISR

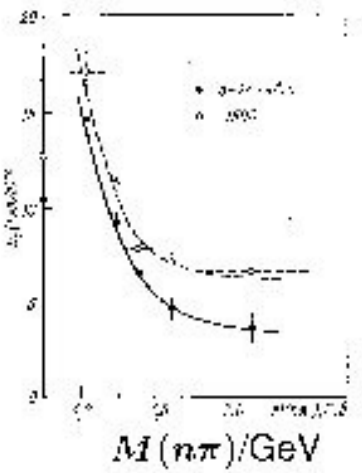

Geometric interpretation: $\langle r^2 \rangle = 2b_1 \cdot (\hbar c)^2 \simeq 2$ fm^2 $\Rightarrow (1.6R_p)^2 \Rightarrow$ ultra-peripheral process

DPP explanation: low mass $\pi^+ n$ state $\to$ large slope, high masses $\to$ less steep slope

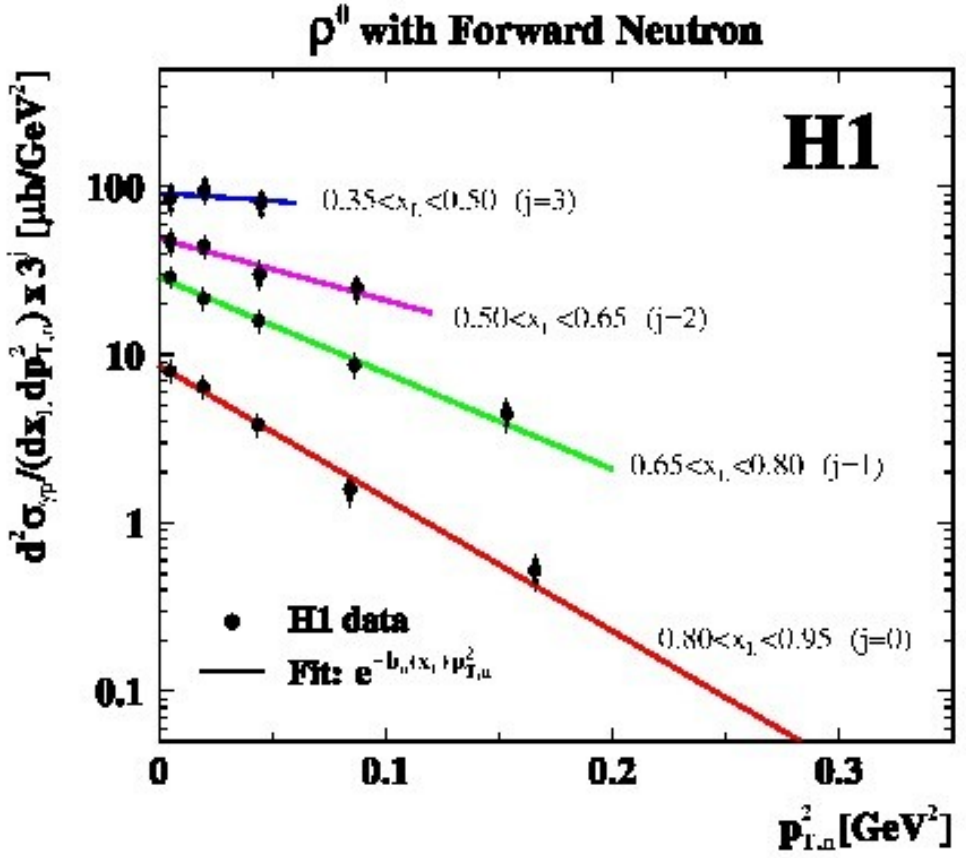

Figure 7: Double differential cross section $d^2\sigma_{\gamma p}/dx_L dp^2_{T,n}$ of neutrons in the range $20 < W_{\gamma p} < 200$ GeV fitted with single exponential functions. The cross sections in different x_L bins j are scaled by the factor 3^j for better visibility. The binning scheme is shown in figure 2c. The data points are shown with statistical (inner error bars) and total (outer error bars) uncertainties excluding an overall normalisation error of 4.4%.

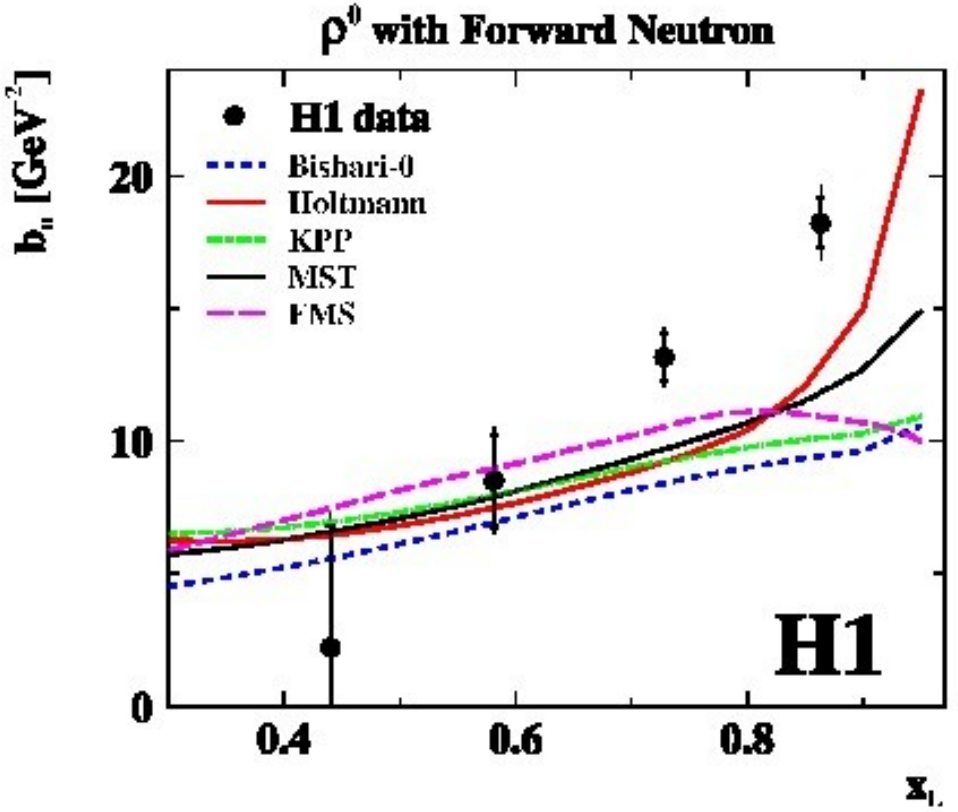

Figure 8: The exponential slopes fitted through the $e^{b_n t}$ dependence of the leading neutrons as a function of x_L. The inner error bars represent statistical errors and the outer error bars are statistical and systematic errors added in quadrature. The data points are compared to the expectations of several parameterisations of the pion flux within the OPE model.

LU TP 15-59
December 2015

Exclusive processes with a leading neutron in ep collisions

V.P. Gonçalves[a], F.S. Navarra[b] and D. Spiering[a]
[a] Department of Theoretical and Nuclear Physics, Lund University, Box 118, SE-221 00 Lund, Sweden
[b] High and Medium Energy Group, Instituto de Física e Química, Universidade Federal de Itajubá
Caixa Postal 351, 37500-903 Itajubá, MG, Brazil.
[c] Instituto de Física, Universidade de São Paulo,
C.P. 66318, 05315-970 São Paulo, SP, Brazil.

In this paper we extend the color dipole formalism to the study of exclusive processes associated with a leading neutron in ep collisions at high energies. The exclusive ρ, ϕ and J/Ψ production is studied in the Deeply Virtual Compton Scattering and analyzed assuming a difference between the color dipole and the photon emitted by the electron proton. We compare our predictions with the HERA data on ρ production and estimate the magnitude of the non-pion contribution. We show that the color dipole formalism is able to describe the current data. Finally, we present our estimates for the exclusive cross section which can be studied at HERA and in future electron-proton colliders.

PACS number: 13.85.-t, 24.85.+p, 25.30.-c
Keywords: Quantum Chromodynamics, Leading Particle Production, Saturation Effects

I. INTRODUCTION

The study of electron - proton (ep) collisions at HERA has improved our understanding of the structure of the proton as well as that of the dynamics of the strong interactions at high energies (For a review see, e.g. Ref. [1]). In particular, the study of diffractive processes has been one of the most successful areas at HERA, with vector meson production and Deeply Virtual Compton Scattering (DVCS) or exclusive processes $ep \to eVp$ with $V = \rho, \phi, J/\Psi, \gamma$ being important probes of the transition between the soft and hard regimes of QCD. These processes have been the subject of intensive theoretical and experimental investigations, with one of the main motivations for these studies being the possibility to probe the QCD dynamics at high energies, driven by the gluon content of the proton which is strongly subject to non-linear effects (parton saturation) [2]. An important lesson from the analysis of the HERA data at small values of the Bjorken x variable is that the inclusive and diffractive processes can be self-consistently described using a unified framework - the color dipole formalism. This approach was proposed many years ago in Ref. [3] and considers that the high energy projectile can be described by a color singlet $q\bar{q}$ configuration, a dipole, and that the interaction of the dipole with the target can be described by the color dipole cross section $\sigma_{dip}(x, r)$, with the transverse size of the dipole r being conserved during the interaction process. In this approach all information about the target and the strong interaction physics is encoded in $\sigma_{dip}(x, r)$, which is determined by the imaginary part of the forward amplitude of the scattering between a small $q\bar{q}$ dipole (a colorless object, multiparton configuration) and a generic hadronic target, denoted by $\mathcal{N}(x, r, b)$, where the dipole size (transverse size given by the vector $r = x - y$, with x and y being the transverse vectors of the quark and antiquark, respectively), and $b = (x+y)/2$ is the impact parameter. In the Color Glass Condensate (CGC) formalism [4, 5], $\mathcal{N}$ contains all the information about non-linear and quantum effects in the hadron wave function. It can be obtained by solving an appropriate evolution equation in the rapidity $Y \equiv \ln(1/x)$, which in its simplest form is the Balitsky-Kovchegov (BK) equation [6, 7]. Alternatively, the scattering amplitude can be obtained using phenomenological models based on saturation physics constructed taking into account the analytical solutions of the BK equation which are valid in the low and high density regimes. As discussed in [7], the combination between the color dipole formalism and saturation physics are quite successful to describe the current and were predict HERA data on the inclusive (reduced cross section) as well as the diffractive processes in a large range of photon-proton center - of - mass energies W, photon virtualities Q^2 and x values.

HERA has also provided high precision experimental data on several exclusive processes $ep \to eVp$ ($V = \rho, \phi, J/\Psi, \gamma$), where the final proton is converted into a neutron via a charge exchange [8]. Very recently the first measurements of

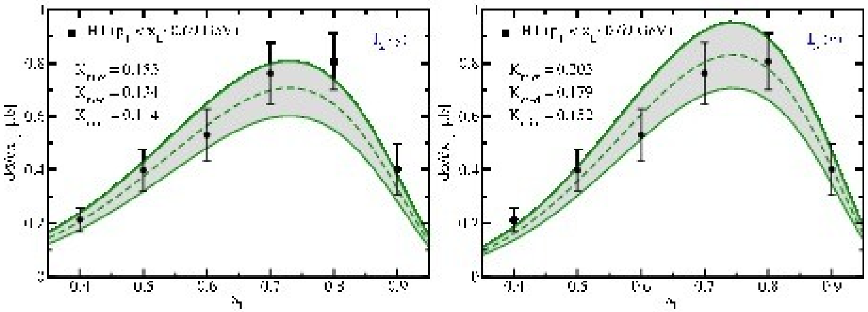

FIG. 6: (Color online) Leading neutron spectra in exclusive ρ photoproduction obtained considering the possible range of values of the K factor fixed using the other set of experimental data and two models for the pion flux. H1 data [9] obtained assuming that $p_T < 0.69 \cdot x_L$ GeV.

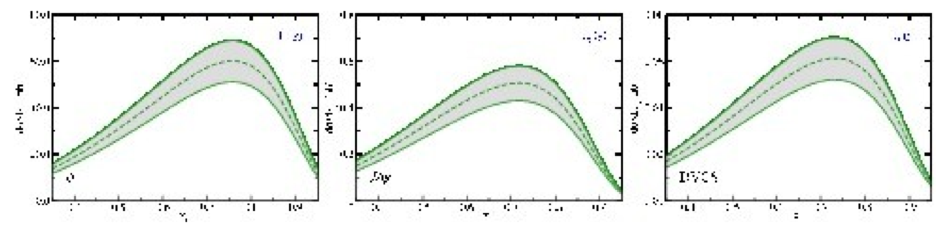

FIG. 7: (Color online) Predictions for the leading neutron spectra in exclusive ϕ, J/Ψ and DVCS production in the HERA kinematical range: $W = 90$ GeV and $p_T < 0.2$ GeV.

sections, the experimental analysis of these using processes associated with a leading neutron is feasible in future ep colliders. In particular, as the cross sections strongly increase when $Q^2 \to 0$, the analysis of the vector meson photoproduction in ep collisions can be useful to understand leading neutron spectra, which are of crucial importance in particle production in cosmic ray physics. Another possibility is the study of this process in ultraperipheral hadronic collisions, with the leading neutron being a tag for exclusive production. In principle, these processes can be studied in the future at the LHC. Such proposition will be discussed in detail in a forthcoming publication.

IV. SUMMARY

One of the important goals in particle physics is to understand the production of leading particles, i.e. the production of baryons which have large fractional longitudinal momentum ($x_L > 0.3$) and the same valence quarks (or at least one of them) as the incoming particles. Recent measurements of the leading neutron spectra in ep collisions at HERA have shed a new light on this subject. However, the description of the semi - inclusive and exclusive leading neutron processes remains without a satisfactory theoretical description. In a previous work [20], we proposed to describe the semi - inclusive leading neutron process using using the color dipole formalism, which successfully describes the inclusive and diffractive HERA data taking into account the QCD dynamics and the non - linear effects which are expected to be present at large energies. Making use of very simple assumptions about the relation between the dipole - pion and the dipole - proton scattering amplitudes and about the absorptive corrections, we demonstrated that the semi - inclusive data can be described by this formalism and that Feynman scaling is expected at large energies. In this paper we have extended our analysis to exclusive processes associated with a leading neutron. Considering the same assumptions used for the semi - inclusive case, we have analysed in detail the dependence of our predictions on the choice of the vector meson wave function, of the dipole model and and of the pion flux. We demonstrated that the HERA data on the exclusive ρ photoproduction associated with a leading neutron can be quite well described

Summary

- Photoproduction cross section for exclusive ρ^0 production associated with leading neutron is measured for the first time at HERA.
- Differential cross sections for the reaction $\gamma p \rightarrow \rho^0 n \pi^+$ exhibit features typical for exclusive double peripheral process.
- The elastic photon-pion cross section, $\sigma(\gamma\pi^- \rightarrow \rho^0\pi^-)$, is extracted in the OPE approximation.

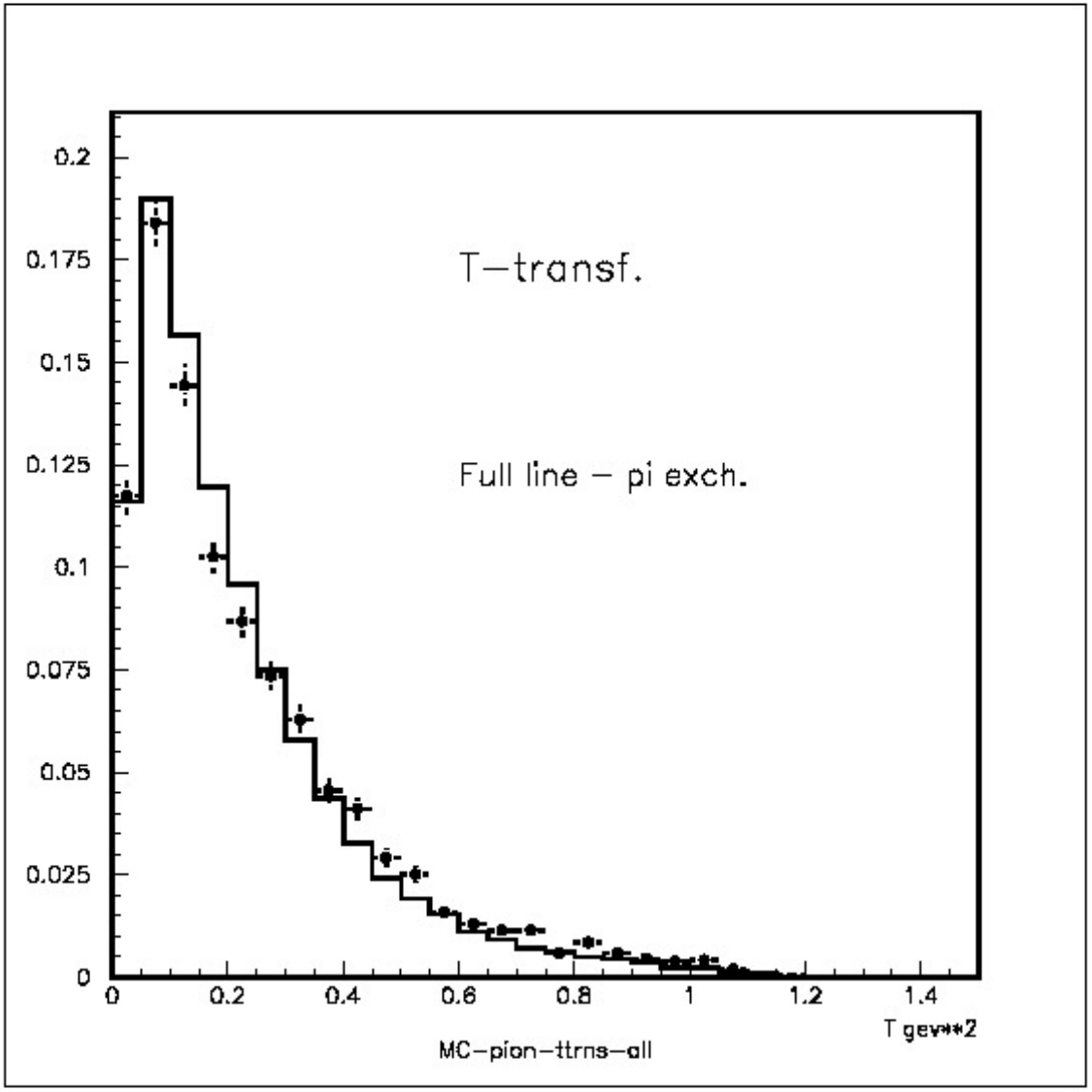
T—transf.
Full line – pi exch.
0.2
0.175
0.15
0.125
0.1
0.075
0.05
0.025
0
0
0.2
0.4
0.6
0.8
1
1.2
1.4
T gev**2
MC-pion-ttrns-all